J. Plasma Physics (2012), *vol.* 78, *part* 1, *pp.* 71–85. © Cambridge University Press 2011
doi:10.1017/S0022377811000420

Double Alfvén waves

G. M. WEBB[1], Q. HU[1], B. DASGUPTA[1] and G. P. ZANK[1,2]

[1]CSPAR, The University of Alabama in Huntsville, Huntsville AL 35805, USA (gmw0002@uah.edu)

[2]Department of Physics, The University of Alabama in Huntsville, Huntsville AL 35899, USA

(Received 5 June 2011; revised 12 September 2011; accepted 19 September 2011; first published online 17 October 2011)

Abstract. Double Alfvén wave solutions of the magnetohydrodynamic equations in which the physical variables (the gas density ρ, fluid velocity $\mathbf{u}$, gas pressure p, and magnetic field induction $\mathbf{B}$) depend only on two independent wave phases $\varphi^1(\mathbf{x},t)$ and $\varphi^2(\mathbf{x},t)$ are obtained. The integrals for the double Alfvén wave are the same as for simple waves, namely, the gas pressure, magnetic pressure, and group velocity of the wave are constant. Compatibility conditions on the evolution of the magnetic field $\mathbf{B}$ due to changes in φ^1 and φ^2, as well as constraints due to Gauss's law $\nabla\cdot\mathbf{B}=0$ are discussed. The magnetic field lines and hodographs of $\mathbf{B}$ in which the tip of the magnetic field $\mathbf{B}$ moves on the sphere $|\mathbf{B}|=B=const.$ are used to delineate the physical characteristics of the wave. Hamilton's equations for the simple Alfvén wave with wave normal $\mathbf{n}(\varphi)$, and with magnetic induction $\mathbf{B}(\varphi)$ in which φ is the wave phase, are obtained by using the Frenet–Serret equations for curves $\mathbf{x}=\mathbf{X}(\varphi)$ in differential geometry. The use of differential geometry of 2D surfaces in a 3D Euclidean space to describe double Alfvén waves is briefly discussed.

1. Introduction

Alfvén waves play an important role in laboratory and fusion plasmas (e.g. Chen and Hasegawa 1974; Hasegawa and Chen 1975; Gekelman et al. 2011). Alfvén waves are also important in space plasmas (e.g. Barnes and Hollweg 1974; Barnes 1976, 1981; Heinemann and Olbert 1980; Matthaeus and Goldstein 1982; Roberts et al. 1987; Zhou and Matthaeus 1990a, 1990b; MacGregor and Charbonneau 1994; Matthaeus et al. 1994; Webb et al. 1996, 2010, 2011; Zank et al. 1996, 2010; Bruno et al. 2001; Bruno and Carbone 2005; Breech et al. 2008; ; Gosling et al. 2009, 2010).

Webb et al. (1996, 2010, 2011) investigated simple Alfvén waves in magnetohydrodynamic (MHD) plasmas, in which the physical variables (density ρ, fluid velocity $\mathbf{u}$, magnetic field induction $\mathbf{B}$, gas pressure p, and entropy S, in the case of MHD) depend only on a single variable $\varphi(x,y,z,t)$. Webb et al. (2010) investigated the relative helicity, Euler potentials, and magnetic field lines for the planar shear Alfvén wave and a basic torsional Alfvén wave solution in which the wave normal describes a circle in the xy-plane, and in which the mean field lies along the z-axis. The torsional wave is a generalization of the centered simple Alfvén wave obtained by Barnes (1976) (in Barnes solution, $B_z=0$). The magnetic helicity of more general simple Alfvén waves obtained by Webb et al. (2010) were discussed in terms of the linkage of the toroidal and poloidal magnetic fluxes in the wave.

Two methods have been used to obtain k-waves (i.e. waves with k independent phases) in fluid dynamics and MHD. The first method is the method of generalized characteristics (GMC), and the second method is the conditional symmetry method (CSM). These two methods do not in general give the same solutions (e.g. Grundland and Huard 2007). The CSM method is more general than the GMC method, but many useful solutions have been obtained by the GMC method.

Grundland and Picard (2004) derived simple waves and double waves in MHD using the CSM. They obtained so-called double entropy (EE) waves for which the eigenvalues in the fluid frame are zero (in some cases the EE wave is associated with a slow magneto-acoustic wave propagating perpendicular to the magnetic field, and would be labelled as a pressure balance structure in space plasma physics), double Alfvén (AA) waves, double Alfvén-entropy (AE) waves, double fast (FF) magnetoacoustic waves, and double fast magnetoacoustic entropy (FE) waves. Our aim is to provide explicit examples of double Alfvén waves.

In Sec. 2 the MHD equations are introduced. Section 3 considers the double Alfvén wave solutions based in part on the work of Grundland and Picard (2004). The double Alfvén waves have two wave phases $\varphi^1(\mathbf{x},t)$ and $\varphi^2(\mathbf{x},t)$, and in general the wave normals $\mathbf{n}^1$ and $\mathbf{n}^2$ can depend on both φ^1 and φ^2, but there are constraints on $\mathbf{n}^1(\varphi^1,\varphi^2)$ and $\mathbf{n}^2(\varphi^1,\varphi^2)$ due to Gauss's law $\nabla\cdot\mathbf{B}=0$. The integrability or compatibility conditions for the φ^1 and φ^2 evolution of $\mathbf{B}$ are determined. Exact analytic solutions for $\mathbf{B}$ are obtained for cases where $\mathbf{n}^1$ and $\mathbf{n}^2$ are constant and independent vectors. Numerical examples are given in Sec. 4. Section 5 outlines extensions of the theory of simple and double Alfvén waves. By using the

https://doi.org/10.1017/S0022377811000420 Published online by Cambridge University Press

Hamiltonian formulation of the Frenet–Serret equations (e.g. Padhye, 1998), a Hamiltonian form of the **B** evolution equations for simple Alfvén waves is developed.

2. The model

The magnetohydrodynamic equations can be written in the following form:

$$\frac{\partial \rho}{\partial t} + \nabla \cdot (\rho \mathbf{u}) = 0, \tag{2.1}$$

$$\frac{\partial}{\partial t}(\rho \mathbf{u}) + \nabla \cdot \left[\rho \mathbf{u}\mathbf{u} + \left(p + \frac{B^2}{2\mu}\right)\mathbf{I} - \frac{\mathbf{B}\mathbf{B}}{\mu}\right] = 0, \tag{2.2}$$

$$\frac{\partial}{\partial t}(\rho S) + \nabla \cdot (\rho \mathbf{u} S) = 0, \tag{2.3}$$

$$\frac{\partial \mathbf{B}}{\partial t} - \nabla \times (\mathbf{u} \times \mathbf{B}) = 0, \tag{2.4}$$

where ρ, $\mathbf{u}$, p, S, and $\mathbf{B}$ correspond to the gas density, fluid velocity, pressure, specific entropy, and magnetic induction $\mathbf{B}$, respectively, and $\mathbf{I}$ is the unit 3×3 dyadic. The gas pressure $p = p(\rho, S)$ is a function of the density ρ and entropy S, and μ is the magnetic permeability. Equations (2.1)–(2.4) are supplemented by Gauss' law,

$$\nabla \cdot \mathbf{B} = 0. \tag{2.5}$$

3. Double Alfvén waves

By using the CSM, Grundland and Picard (2004) obtained double wave solutions of the MHD equations, including double Alfvén waves. The integrals for the double Alfvén wave are the same as for the simple Alfvén wave. For the forward Alfvén wave case, the integrals are

$$\mathbf{u} + \frac{\mathbf{B}}{\sqrt{\mu\rho}} \equiv \mathbf{u} + \mathbf{V}_A = (V_1, V_2, V_3) = const., \quad p = c_4,$$

$$\rho = c_5, \quad B^2 = c_6, \tag{3.1}$$

where $V_1, V_2, V_3, c_4, c_5,$ and c_6 are constants. However, the Alfvén double wave, has two phase variables φ^1 and φ^2, which are independent functions of (t, x, y, z), whereas the simple Alfvén wave depends on a single phase variable $\varphi(t, x, y, z)$. The phase variables are given implicitly by equations of the following form:

$$\varphi^1 = \mathbf{n}^1(\varphi^1, \varphi^2) \cdot \tilde{\mathbf{x}}, \quad \varphi^2 = \mathbf{n}^2(\varphi^1, \varphi^2) \cdot \tilde{\mathbf{x}}, \quad \tilde{\mathbf{x}} = \mathbf{x} - \mathbf{V}t, \tag{3.2}$$

where the wave normals $\mathbf{n}^1(\varphi^1, \varphi^2)$ and $\mathbf{n}^2(\varphi^1, \varphi^2)$ must be chosen to satisfy

$$\mathbf{n}^1 \cdot \frac{\partial \mathbf{B}}{\partial \varphi^1} = 0, \quad \mathbf{n}^2 \cdot \frac{\partial \mathbf{B}}{\partial \varphi^2} = 0, \tag{3.3}$$

in order to satisfy Gauss's law $\nabla \cdot \mathbf{B} = 0$. Grundland and Picard (2004) used $\mathbf{n}^1 = \mathbf{n}^1(\varphi^1, \varphi^2)$ and $\mathbf{n}^2 = \mathbf{n}^2(\varphi^1, \varphi^2)$ in (3.2) and (3.3), but these forms for $\mathbf{n}^1$ and $\mathbf{n}^2$ must be constrained to ensure $\nabla \cdot \mathbf{B} = 0$. The conditions $\nabla\varphi^1 \cdot \partial\mathbf{B}/\partial\varphi^1 = 0$ and $\nabla\varphi^2 \cdot \partial\mathbf{B}/\partial\varphi^2 = 0$ together ensure $\nabla \cdot \mathbf{B} = 0$. If $\mathbf{n}^1 = \mathbf{n}^1(\varphi^1)$ and $\mathbf{n}^2 = \mathbf{n}^2(\varphi^2)$, conditions (3.3) ensure that $\nabla \cdot \mathbf{B} = 0$. These constraints and integrability conditions for double Alfvén waves are discussed in Sec. 3.1. For double waves, the state vector $\mathbf{W} = (\rho, \mathbf{u}, \mathbf{B}, p)$ depends only on the Riemann invariants φ^1 and φ^2, and is time-independent in the frame moving with velocity $\mathbf{V}$.

One can replace (3.2) by the following equations:

$$f^1(\varphi^1) = \mathbf{n}^1(\varphi^1, \varphi^2) \cdot \tilde{\mathbf{x}} \quad \text{and} \quad f^2(\varphi^2) = \mathbf{n}^2(\varphi^1, \varphi^2) \cdot \tilde{\mathbf{x}}. \tag{3.4}$$

Centered double waves are obtained for $f^1 = 0$ and/or $f^2 = 0$. However, these solutions exhibit gradient catastrophe at $\mathbf{x} = 0$. Non-centered simple Alfvén waves also exhibit gradient catastrophe where the current density $\mathbf{J} = \nabla \times \mathbf{B}/\mu_0$ diverges, but not at $\mathbf{x} = 0$.

The double Alfvén wave described by (3.1), (3.2), and (3.4) satisfies the MHD equations provided that the matrix

$$\psi^i_j = \frac{df^i(\varphi^i)}{d\varphi^i}\delta^i_j - \tilde{x}^\mu \frac{\partial n^i_\mu}{\partial \varphi^j} \quad i, j = 1, 2 \tag{3.5}$$

is non-singular (i.e. $\det(\psi^i_j) \neq 0$). The double wave solutions (3.1)–(3.3) have wave vectors in the frame in which the wave has velocity $\mathbf{V}$ of the forms

$$\kappa^0_\mu = [-\mathbf{V} \cdot \mathbf{n}^1(\varphi^1, \varphi^2), \mathbf{n}^1(\varphi^1, \varphi^2)],$$

$$\kappa^1_\mu = [-\mathbf{V} \cdot \mathbf{n}^2(\varphi^1, \varphi^2), \mathbf{n}^2(\varphi^1, \varphi^2)]. \tag{3.6}$$

In the group velocity frame $\mathbf{V} = 0$.

We verify solution (3.1), (3.2), or (3.4) with $\det(\psi^i_j) \neq 0$ and $\nabla \cdot \mathbf{B} = 0$ below. We work in the group velocity frame $\tilde{\Sigma}$ in which $\tilde{\mathbf{x}} = \mathbf{x} - \mathbf{V}t$ are the spatial coordinates. In this frame, the solutions are time-independent. Implicit differentiation of (3.4) gives

$$\frac{\partial \varphi^c}{\partial \tilde{x}^\mu} = (\Psi^{-1})^{\mathsf{c}}_{\mathsf{s}} \mathsf{n}^{\mathsf{s}}_\mu. \tag{3.7}$$

The physical variables $\mathbf{W} = (\rho, \mathbf{u}, \mathbf{B}, p)$ have following derivatives:

$$\frac{\partial w^v}{\partial \tilde{x}^\alpha} = \frac{\partial w^v}{\partial \varphi^s}\frac{\partial \varphi^s}{\partial \tilde{x}^\alpha} \equiv \frac{\partial w^v}{\partial \varphi^s}(\Psi^{-1})^{\mathsf{s}}_{\mathsf{c}} \mathsf{n}^{\mathsf{c}}_\alpha. \tag{3.8}$$

3.1. *The condition* $\nabla \cdot \mathbf{B} = 0$ *and compatibility conditions*

To compute $\nabla \cdot \mathbf{B}$ we first consider the form of ψ^i_j. From (3.5) we obtain

$$\psi^1_1 = \frac{df^1}{d\varphi^1} - \tilde{x}^\mu \frac{\partial n^1_\mu}{\partial \varphi^1}, \quad \psi^2_2 = \frac{df^2}{d\varphi^2} - \tilde{x}^\mu \frac{\partial n^2_\mu}{\partial \varphi^2},$$

$$\psi^1_2 = -\tilde{x}^\mu \frac{\partial n^1_\mu}{\partial \varphi^2}, \quad \psi^2_1 = -\tilde{x}^\mu \frac{\partial n^2_\mu}{\partial \varphi^1}. \tag{3.9}$$

The determinant of the matrix Ψ in (3.9) is

$$\Delta = \det(\Psi) = \psi^1_1\psi^2_2 - \psi^1_2\psi^2_1$$

$$= \frac{df^1}{d\varphi^1}\frac{df^2}{d\varphi^2} - \tilde{x}^\mu\left(\frac{\partial n^1_\mu}{\partial \varphi^1}\frac{df^2}{d\varphi^2} + \frac{\partial n^2_\mu}{\partial \varphi^2}\frac{df^1}{d\varphi^1}\right)$$

$$+\tilde{x}^\mu\tilde{x}^\alpha\left(\frac{\partial n^1_\alpha}{\partial \varphi^1}\frac{\partial n^2_\mu}{\partial \varphi^2} - \frac{\partial n^1_\alpha}{\partial \varphi^2}\frac{\partial n^2_\mu}{\partial \varphi^1}\right). \tag{3.10}$$

https://doi.org/10.1017/S0022377811000420 Published online by Cambridge University Press

Using the inverse of the 2×2 matrix Ψ we obtain

$$\nabla \cdot \mathbf{B} = \nabla\varphi^1 \cdot \frac{\partial \mathbf{B}}{\partial \varphi^1} + \nabla\varphi^2 \cdot \frac{\partial \mathbf{B}}{\partial \varphi^2}$$

$$\equiv \frac{\partial B^i}{\partial \varphi^1}(\Psi^{-1})^1_{\mathsf{c}}\mathsf{n}^{\mathsf{c}}_{\mathsf{i}} + \frac{\partial \mathsf{B}^{\mathsf{i}}}{\partial \varphi^2}(\Psi^{-1})^2_{\mathsf{c}}\mathsf{n}^{\mathsf{c}}_{\mathsf{i}}, \quad (3.11)$$

which reduces to

$$\nabla \cdot \mathbf{B} = \frac{1}{\Delta}\left(\psi^1_2 \mathbf{n}^1 \cdot \frac{\partial \mathbf{B}}{\partial \varphi^1} + \psi^1_1 \mathbf{n}^2 \cdot \frac{\partial \mathbf{B}}{\partial \varphi^2} - \psi^2_1 \mathbf{n}^1 \cdot \frac{\partial \mathbf{B}}{\partial \varphi^2} - \psi^1_2 \mathbf{n}^2 \cdot \frac{\partial \mathbf{B}}{\partial \varphi^1}\right). \quad (3.12)$$

Imposing the conditions (3.3), (3.12) reduces to

$$\nabla \cdot \mathbf{B} = \frac{1}{\Delta}\left[\tilde{\mathbf{x}} \cdot \frac{\partial \mathbf{n}^2}{\partial \varphi^1}\mathbf{n}^1 \cdot \frac{\partial \mathbf{B}}{\partial \varphi^2} + \tilde{\mathbf{x}} \cdot \frac{\partial \mathbf{n}^1}{\partial \varphi^2}\mathbf{n}^2 \cdot \frac{\partial \mathbf{B}}{\partial \varphi^1}\right]. \quad (3.13)$$

Note $\nabla \cdot \mathbf{B} = 0$ in (3.13) if $\partial \mathbf{n}^2/\partial\varphi^1 = \partial \mathbf{n}^1/\partial\varphi^2 = 0$. In that case, $\mathbf{n}^1 = \mathbf{n}^1(\varphi^1)$ and $\mathbf{n}^2 = \mathbf{n}^2(\varphi^2)$. However, this is not the only possibility. Using (3.3) and noting that $|\mathbf{B}|^2 = const.$, for Alfvén wave solutions, it follows that

$$\frac{\partial \mathbf{B}}{\partial \varphi^1} = \mu \mathbf{n}^1 \times \mathbf{B} \quad \text{and} \quad \frac{\partial \mathbf{B}}{\partial \varphi^2} = \nu \mathbf{n}^2 \times \mathbf{B}, \quad (3.14)$$

where μ and ν are functions of φ^1 and φ^2. Note μ in this section does not refer to the magnetic permeability. Using (3.14) we obtain

$$\mathbf{n}^1 \cdot \frac{\partial \mathbf{B}}{\partial \varphi^2} = \nu \mathbf{B} \cdot \mathbf{n}^1 \times \mathbf{n}^2, \quad \mathbf{n}^2 \cdot \frac{\partial \mathbf{B}}{\partial \varphi^1} = -\mu \mathbf{B} \cdot \mathbf{n}^1 \times \mathbf{n}^2. \quad (3.15)$$

Thus, expression (3.13) for $\nabla \cdot \mathbf{B}$ then reduces to

$$\nabla \cdot \mathbf{B} = \frac{\mathbf{B} \cdot \mathbf{n}^1 \times \mathbf{n}^2}{\Delta}\tilde{\mathbf{x}} \cdot \left(\nu \frac{\partial \mathbf{n}^2}{\partial \varphi^1} - \mu \frac{\partial \mathbf{n}^1}{\partial \varphi^2}\right). \quad (3.16)$$

Thus, $\nabla \cdot \mathbf{B} = 0$ if

$$\mathbf{B} \cdot \mathbf{n}^1 \times \mathbf{n}^2 = 0, \quad (3.17)$$

or if

$$\nu \frac{\partial \mathbf{n}^2}{\partial \varphi^1} - \mu \frac{\partial \mathbf{n}^1}{\partial \varphi^2} = 0. \quad (3.18)$$

Both possibilities (3.17) and (3.18) allow for solutions for double Alfvén waves, in which the wave normals $\mathbf{n}^1$ and $\mathbf{n}^2$ can be functions of φ^1 and φ^2.

Equations (3.14) can be written as

$$\frac{\partial \mathbf{B}}{\partial \varphi^1} = \Lambda^1 \mathbf{B} \equiv \mathbf{N}^1 \times \mathbf{B}, \quad \frac{\partial \mathbf{B}}{\partial \varphi^2} = \Lambda^2 \mathbf{B} \equiv \mathbf{N}^2 \times \mathbf{B}, \quad (3.19)$$

where

$$\mathbf{N}^1 = \mu \mathbf{n}^1, \quad \mathbf{N}^2 = \nu \mathbf{n}^2. \quad (3.20)$$

The matrices Λ^1 and Λ^2 are dual to the vectors $\mathbf{N}^1$ and $\mathbf{N}^2$ and are related by

$$\Lambda^1_{ik} = -\varepsilon_{ikj}N^1_j, \quad \Lambda^2_{ik} = -\varepsilon_{ikj}N^2_j,$$

$$N^1_s = -\frac{1}{2}\varepsilon_{sik}\Lambda^1_{ik}, \quad N^2_s = -\frac{1}{2}\varepsilon_{sik}\Lambda^2_{ik}. \quad (3.21)$$

The integrability conditions for (3.19), namely

$$\frac{\partial^2 \mathbf{B}}{\partial \varphi^1 \partial \varphi^2} = \frac{\partial^2 \mathbf{B}}{\partial \varphi^2 \partial \varphi^1}, \quad (3.22)$$

reduce to the matrix equation

$$\left\{\frac{\partial \Lambda^1}{\partial \varphi^2} - \frac{\partial \Lambda^2}{\partial \varphi^1} + [\Lambda^1, \Lambda^2]\right\}\mathbf{B} = 0, \quad (3.23)$$

where

$$[\Lambda^1, \Lambda^2] = \Lambda^1\Lambda^2 - \Lambda^1\Lambda^2 \quad (3.24)$$

is the matrix commutator of Λ^1 and Λ^2.

Noting that

$$\Lambda^1 \mathbf{B} = \mathbf{N}^1 \times \mathbf{B}, \quad \Lambda^2 \mathbf{B} = \mathbf{N}^2 \times \mathbf{B}, \quad (3.25)$$

the matrix equation (3.23) reduces to the vector equation

$$\left(\frac{\partial \mathbf{N}^1}{\partial \varphi^2} - \frac{\partial \mathbf{N}^2}{\partial \varphi^1} + \mathbf{N}^1 \times \mathbf{N}^2\right) \times \mathbf{B} = 0. \quad (3.26)$$

The compatibility condition (3.26) is equivalent to the following equation:

$$\mathbf{B} = \lambda \mathbf{C}, \quad \text{where} \quad \mathbf{C} = \frac{\partial \mathbf{N}^1}{\partial \varphi^2} - \frac{\partial \mathbf{N}^2}{\partial \varphi^1} + \mathbf{N}^1 \times \mathbf{N}^2, \quad (3.27)$$

and $\lambda(\varphi^1, \varphi^2)$ is a scalar function of φ^1 and φ^2. Thus, $\mathbf{B}$ must be parallel to $\mathbf{C}$ in (3.27) in order that the φ^1 and φ^2 evolutions in (3.19) are compatible. Thus, the solution for $\mathbf{B}$ is delimited by the wave normals $\mathbf{N}^1$ and $\mathbf{N}^2$ and the torsion coefficients μ and ν. The condition (3.18) must be satisfied to ensure $\nabla \cdot \mathbf{B} = 0$.

Using (3.18), the vector $\mathbf{C}$ in (3.27) can be written in the following form:

$$\mathbf{C} = \frac{\partial \ln(\mu)}{\partial \varphi^2}\mathbf{N}^1 - \frac{\partial \ln(\nu)}{\partial \varphi^1}\mathbf{N}^2 + \mathbf{N}^1 \times \mathbf{N}^2$$

$$\equiv \frac{\partial \mu}{\partial \varphi^2}\mathbf{n}^1 - \frac{\partial \nu}{\partial \varphi^1}\mathbf{n}^2 + \mu\nu \mathbf{n}^1 \times \mathbf{n}^2. \quad (3.28)$$

Equations (3.27) and (3.28) are the integrability conditions for smooth solutions.

There is also the possibility that the matrix equation,

$$\frac{\partial \Lambda^1}{\partial \varphi^2} - \frac{\partial \Lambda^2}{\partial \varphi^1} + [\Lambda^1, \Lambda^2] = 0, \quad (3.29)$$

is satisfied identically independent of $\mathbf{B}$. Equation (3.29) is known as zero curvature equation in the theory of integrable systems.

An inspection of the equation $\mathbf{C} = 0$, where $\mathbf{C}$ is given by (3.28), assuming $\mathbf{n}^1$ and $\mathbf{n}^2$ are independent vectors, leads to the equations $\partial\mu/\partial\varphi^2 = \partial\nu/\partial\varphi^1 = 0$ and $\mu\nu = 0$, which imply the simple wave case in which there is only one wave phase. Thus, the compatibility condition (3.27) must apply with $\lambda \neq 0$, which implies that the unit vector along the magnetic field is given by $\hat{\mathbf{C}} = \mathbf{C}/|\mathbf{C}|$.

Solution verification

The mass continuity equation, the MHD momentum equation, and Faraday's equation are satisfied for the double Alfvén wave. These results may be verified by using the wave frame $\tilde{\Sigma}$ moving with constant velocity $\mathbf{V}$, in which $\tilde{\mathbf{u}} = \mathbf{u} - \mathbf{V} = -\mathbf{V}_A$. In $\tilde{\Sigma}$, $\nabla \cdot (\rho\tilde{\mathbf{u}}) = 0$ as $\tilde{\mathbf{u}} = -\mathbf{B}/\sqrt{\mu\rho}$, $\rho = const.$, and $\nabla \cdot \mathbf{B} = 0$. Similarly, the

https://doi.org/10.1017/S0022377811000420 Published online by Cambridge University Press

momentum equation and Faraday's equations reduce to the forms

$$\rho\tilde{\mathbf{u}}\cdot\nabla\tilde{\mathbf{u}}=\frac{\mathbf{B}\cdot\nabla\mathbf{B}}{\mu},\quad \nabla\times(\tilde{\mathbf{u}}\times\mathbf{B})=0, \tag{3.30}$$

which are satisfied as $\tilde{\mathbf{u}}=-\mathbf{B}/\sqrt{\mu\rho}$. For $p=const.$ and $\rho=const.$, the entropy is constant and the entropy advection equation is satisfied.

3.2. Examples

Consider the case where the wave normals $\mathbf{n}^1$ and $\mathbf{n}^2$ in (3.2) are constant unit vectors. There are clearly more complicated solutions of (3.19) in which the wave normals are functions of φ^1 and φ^2. The solutions for $\mathbf{n}^1$ and $\mathbf{n}^2$ constants are a useful simple class of solutions.

By choosing

$$\varphi^1=\mathbf{n}^1\cdot\tilde{\mathbf{x}}\quad\text{and}\quad\varphi^2=\mathbf{n}^2\cdot\tilde{\mathbf{x}}, \tag{3.31}$$

where $\mathbf{n}^1$ and $\mathbf{n}^2$ are constant unit vectors, conditions (3.3) ensure $\nabla\cdot\mathbf{B}=0$. Noting $B^2=c_6$ is constant implies

$$\mathbf{n}^1\cdot\frac{\partial\mathbf{B}}{\partial\varphi^1}=\frac{\partial(\mathbf{n}^1\cdot\mathbf{B})}{\partial\varphi^1}=0,\quad \mathbf{n}^2\cdot\frac{\partial\mathbf{B}}{\partial\varphi^2}=\frac{\partial(\mathbf{n}^2\cdot\mathbf{B})}{\partial\varphi^2}=0, \tag{3.32}$$

and hence

$$\mathbf{n}^1\cdot\mathbf{e}_B=g(\varphi^2),\quad \mathbf{n}^2\cdot\mathbf{e}_B=h(\varphi^1), \tag{3.33}$$

where $\mathbf{e}_B=\mathbf{B}/B$ is the magnetic field unit vector and $g(\varphi^1)$ and $h(\varphi^1)$ are functions of φ^2 and φ^1, respectively (we restrict $g(\varphi^2)$ and $h(\varphi^1)$ such that $|h|<1$ and $|g|<1$).

It follows that the general solution for $\mathbf{B}$ has the following form:

$$\mathbf{B}=B(\tilde{B}_1\mathbf{n}^1+\tilde{B}_2\mathbf{n}^2+\tilde{B}_3\mathbf{a}_3)=B\mathbf{e}_B, \tag{3.34}$$

where

$$\mathbf{a}_3=\frac{\mathbf{n}^1\times\mathbf{n}^2}{|\mathbf{n}^1\times\mathbf{n}^2|}. \tag{3.35}$$

Note $\mathbf{n}^1$, $\mathbf{n}^2$, and $\mathbf{a}_3$ are not in general orthonormal unit vectors. From (3.33)–(3.35) we obtain

$$\tilde{B}_1=\frac{[g(\varphi^2)-\mathbf{n}^1\cdot\mathbf{n}^2h(\varphi^1)]}{\Delta},\quad \tilde{B}_2=\frac{[h(\varphi^1)-\mathbf{n}^1\cdot\mathbf{n}^2g(\varphi^2)]}{\Delta},$$

$$\tilde{B}_3=\sigma\left[1-\left(\frac{g^2+h^2-2hg\mathbf{n}^1\cdot\mathbf{n}^2}{\Delta}\right)\right]^{1/2},\quad\text{where}$$

$$\sigma=\pm1, \tag{3.36}$$

and

$$\Delta=1-(\mathbf{n}^1\cdot\mathbf{n}^2)^2. \tag{3.37}$$

The latter formula for $\tilde{B}_3$ arises from requiring $\mathbf{e}_B\cdot\mathbf{e}_B=1$.

3.2.1. Contravariant and covariant forms for $\mathbf{B}$. The solutions (3.34)–(3.37) can be expressed in the contravariant form:

$$\mathbf{B}=B^\alpha\mathbf{e}_\alpha=B[g(\varphi^2)\mathbf{e}_1+h(\varphi^1)\mathbf{e}_2+k(\varphi^1,\varphi^2)\mathbf{e}_3], \tag{3.38}$$

or in the covariant form:

$$\mathbf{B}=B_\alpha\omega^\alpha\equiv B_\alpha\nabla\varphi^\alpha, \tag{3.39}$$

where

$$\varphi^1=\mathbf{n}^1\cdot\tilde{\mathbf{x}},\quad\varphi^2=\mathbf{n}^2\cdot\tilde{\mathbf{x}},\quad\varphi^3=\mathbf{n}^3\cdot\tilde{\mathbf{x}},\quad\mathbf{n}^3=\mathbf{n}^1\times\mathbf{n}^2,$$

$$\omega^\alpha=\nabla\varphi^\alpha\equiv\mathbf{n}^\alpha,\quad\mathbf{e}_\alpha=\frac{\partial\mathbf{x}}{\partial\varphi^\alpha},\quad\alpha=1,2,3. \tag{3.40}$$

Here the $\{\mathbf{e}_\alpha\}$ are contravariant base vectors and the $\{\omega^\alpha\}$ are dual covariant base vectors. In more general cases where the normals $\mathbf{n}^1$, $\mathbf{n}^2$, and $\mathbf{n}^3$ depend on φ^1 and φ^2, $\omega^\alpha\neq\mathbf{n}^\alpha$. We have introduced a new independent variable φ^3 in (3.40). However, the final solution for $\mathbf{B}$ does not depend on φ^3.

The contravariant components of $\mathbf{B}$ are

$$B^1=Bg(\varphi^2),\quad B^2=Bh(\varphi^1),\quad B^3=Bk(\varphi^1,\varphi^2),$$

$$k(\varphi^1,\varphi^2)=[\Delta-(h^2+g^2-2hg\cos\Theta)]^{1/2},$$

$$\cos\Theta=\mathbf{n}^1\cdot\mathbf{n}^2. \tag{3.41}$$

The contravariant base vectors are given by

$$\mathbf{e}_1=\frac{\mathbf{n}^1-\mathbf{n}^2\cos\Theta}{\Delta},\quad\mathbf{e}_2=\frac{\mathbf{n}^2-\mathbf{n}^1\cos\Theta}{\Delta},\quad\mathbf{e}_3=\frac{\mathbf{n}^3}{\Delta},$$

$$\Delta=1-(\mathbf{n}^1\cdot\mathbf{n}^2)^2\equiv\sin^2\Theta. \tag{3.42}$$

The contravariant form of $\mathbf{B}$ in (3.38) clearly shows the arbitrary functions $h(\varphi^1)$ and $g(\varphi^2)$ in the solution for $\mathbf{B}$.

The covariant components of $\mathbf{B}$ are

$$B_1=\frac{B[g(\varphi^2)-h(\varphi^1)\cos\Theta]}{\Delta},$$

$$B_2=\frac{B[h(\varphi^1)-g(\varphi^2)\cos\Theta]}{\Delta},\quad B_3=\frac{Bk(\varphi^1,\varphi^2)}{\Delta}. \tag{3.43}$$

These components are the same as in (3.36) and (3.37) except that $B_3=B\tilde{B}_3/\sqrt{\Delta}$.

Below, we derive (3.38)–(3.43). The covariant base $\omega^\alpha=\nabla\varphi^\alpha$ follows from the definition (3.40) for the φ^α. To establish the contravariant base $\{\mathbf{e}_\alpha:\ \alpha=1,2,3\}$, we write

$$\mathbf{x}=q_1\mathbf{n}^1+q_2\mathbf{n}^2+q_3\mathbf{n}^3. \tag{3.44}$$

Taking the scalar product of (3.44) with $\mathbf{n}^1$, $\mathbf{n}^2$, and $\mathbf{n}^3$ gives

$$\varphi^1=q_1+q_2\cos\Theta,\quad\varphi^2=q_2+q_1\cos\Theta,$$

$$\varphi^3=q_3\sin^2\Theta\equiv q_3\Delta, \tag{3.45}$$

where $\cos\theta=\mathbf{n}^1\cdot\mathbf{n}^2$. Inversion of (3.45) gives

$$q_1=\frac{\varphi^1-\cos\Theta\varphi^2}{\Delta},\quad q_2=\frac{\varphi^2-\varphi^1\cos\Theta}{\Delta},\quad q_3=\frac{\varphi^3}{\Delta}. \tag{3.46}$$

From (3.44) and (3.46) we obtain

$$\mathbf{e}_\alpha=\frac{\partial\mathbf{x}}{\partial\varphi^\alpha}=\frac{\partial q_1}{\partial\varphi^\alpha}\mathbf{n}^1+\frac{\partial q_2}{\partial\varphi^\alpha}\mathbf{n}^2+\frac{\partial q_3}{\partial\varphi^\alpha}\mathbf{n}^3. \tag{3.47}$$

Using (3.46) and (3.47) gives the results (3.42) for $\mathbf{e}_1,\mathbf{e}_2$, and $\mathbf{e}_3$.

https://doi.org/10.1017/S0022377811000420 Published online by Cambridge University Press

The covariant and contravariant forms of the metric tensor are

$$g_{\alpha\beta} = \mathbf{e}_\alpha \cdot \mathbf{e}_\beta, \quad g^{\alpha\beta} = \omega^\alpha \cdot \omega^\beta. \tag{3.48}$$

For example,

$$g_{\alpha\beta} = \frac{1}{\Delta}\begin{pmatrix} 1 & -\cos\Theta & 0 \\ -\cos\Theta & 1 & 0 \\ 0 & 0 & 1 \end{pmatrix}. \tag{3.49}$$

The matrix $g^{\alpha\beta}$ is the inverse of $g_{\alpha\beta}$. Furthermore, one can establish the relations

$$\omega^i \times \omega^j = \frac{1}{\sqrt{g}}\varepsilon_{ijk}\mathbf{e}_k, \quad \mathbf{e}_i \times \mathbf{e}_j = \sqrt{g}\varepsilon_{ijk}\omega^k, \tag{3.50}$$

between the two bases (e.g. Webb and Zank 2007), where $g = \det(g_{\alpha\beta})$ is the determinant of the metric tensor.

3.2.2. μ, ν, and λ and compatibility conditions. The compatibility conditions of Sec. 4.1 imply that the solution for **B** can be written in the form

$$\mathbf{B} = \lambda\mathbf{C} = \lambda\left[\frac{\partial\mu}{\partial\varphi^2}\mathbf{n}^1 - \frac{\partial\nu}{\partial\varphi^1}\mathbf{n}^2 + \mu\nu\mathbf{n}^3\right], \tag{3.51}$$

where $\lambda^2 = B^2/(\mathbf{C}\cdot\mathbf{C})$.

For the solution (3.34)–(3.37) or (3.38) for **B**, it is straightforward to show that

$$\mu = -\frac{\partial h/\partial\varphi^1}{k(\varphi^1,\varphi^2)}, \quad \nu = \frac{\partial g/\partial\varphi^2}{k(\varphi^1,\varphi^2)},$$

$$\lambda = -\frac{B}{\Delta}\frac{k(\varphi^1,\varphi^2)^3}{\partial h/\partial\varphi^1\partial g/\partial\varphi^2} \equiv \frac{B}{\Delta}\frac{k}{\mu\nu}, \tag{3.52}$$

and the compatibility conditions (3.27) and (3.28) are satisfied. Note that even in the case of constant wave normals, the torsion coefficients μ and ν are non-trivial.

4. Numerical examples

Consider the special case of the above solution with

$$\mathbf{n}^1 = \mathbf{e}_x, \quad \mathbf{n}^2 = \mathbf{e}_y, \quad \mathbf{a}_3 = \mathbf{e}_z, \tag{4.1}$$

where $\mathbf{e}_x$, $\mathbf{e}_y$, and $\mathbf{e}_z$ refer to the unit vectors along x, y, and z axes. We obtain

$$\varphi^1 = x, \quad \varphi^2 = y,$$

$$\mathbf{B} = B[g(y), h(x), \sigma\{1 - g^2(y) - h^2(x)\}^{1/2}], \tag{4.2}$$

where x and y (in an abuse of mathematical notation) now refer to the position in the wave frame, $\sigma = \pm 1$, and we assume $g^2(y) + h^2(x) < 1$. Notice that $\nabla\cdot\mathbf{B} = 0$ and $B^2 = const.$ If we further choose

$$g(y) = \frac{1}{\sqrt{2}}\cos(k_2 y), \quad h(x) = \frac{1}{\sqrt{2}}\cos(k_1 x), \tag{4.3}$$

then we obtain the following magnetic field solution:

$$\mathbf{B} = \frac{B}{\sqrt{2}}[\cos(k_2 y), \cos(k_1 x), \sigma\{\sin^2(k_2 y) + \sin^2(k_1 x)\}^{1/2}]. \tag{4.4}$$

As $k_2 \to 0$ in (4.4), we obtain

$$\mathbf{B} = \frac{B}{\sqrt{2}}\left[1, \cos(k_1 x), \sigma\sin(k_1 x)\right], \tag{4.5}$$

which is a simple shear wave propagating along the x-axis. Similarly, if $k_1 \to 0$ in (4.4), we obtain

$$\mathbf{B} = \frac{B}{\sqrt{2}}\left[\cos(k_2 y), 1, \sigma\sin(k_2 y)\right], \tag{4.6}$$

which corresponds to a simple shear Alfvén wave propagating along the y-axis.

The magnetic field lines for the double wave (4.4) are

$$\frac{dx}{B_x} = \frac{dy}{B_y} = \frac{dz}{B_z}. \tag{4.7}$$

Equations (4.7) have integrals:

$$\frac{\sin(k_1 x)}{k_1} - \frac{\sin(k_2 y)}{k_2} = \eta, \tag{4.8}$$

$$z - \sigma\int^x \frac{\left[\sin^2(k_1 x) + k_2^2(\sin(k_1 x)/k_1 - \eta)^2\right]^{1/2}}{\sigma_y\left[1 - k_2^2(\sin(k_1 x)/k_1 - \eta)^2\right]^{1/2}}dx = \zeta, \tag{4.9}$$

where $\sigma = \mathrm{sgn}(B_z)$ and $\sigma_y = \mathrm{sgn}[\cos(k_2 y)]$. Clearly, $|\eta| < \eta_{\max}$, where $\eta_{\max} = 1/k_1 + 1/k_2$. The intersection of the $\eta = const.$ and $\zeta = const.$ surfaces gives the field line. Note that $\mathbf{B} = \nabla\times\mathbf{A}$, where $\mathbf{A} = (B/\sqrt{2})\zeta\nabla\eta$ is a representation of **B** in terms of the magnetic vector potential **A**.

Case $k_1 = k_2 = k$

For the case $k_1 = k_2 = k$, the field line integrals can be written in the following form:

$$2\sin\tilde{x}\cos\tilde{y} = k\eta = \tilde{\eta}, \tag{4.10}$$

$$z + \frac{1}{\sqrt{2}k}\int^c \frac{(1 - c^2 - \tilde{\eta}^2 c)\sigma}{(1-c)\sqrt{P_4(c)}}dc = \zeta, \tag{4.11}$$

where $\tilde{\eta}$ and ζ are field line integration constants and

$$\tilde{x} = \frac{k(x-y)}{2}, \quad \tilde{y} = \frac{k(x+y)}{2}, \quad \sigma = \mathrm{sgn}[\sin\tilde{y}\cos\tilde{x}],$$

$$c = \cos(2\tilde{x}), \tag{4.12}$$

$$P_4(c) = (c+1)[c - (1 - \tilde{\eta}^2/2)](c^2 + \tilde{\eta}^2 c - 1). \tag{4.13}$$

The field line integral (4.11) is an elliptic integral. Note that

$$P_4(c) = (c+1)(c-c_1)(c-c_2)(c-c_3), \tag{4.14}$$

where

$$c_1 = -\frac{1}{2}[\tilde{\eta}^2 + (\tilde{\eta}^4 + 4)^{1/2}], \quad c_2 = \frac{1}{2}[(\tilde{\eta}^4 + 4)^{1/2} - \tilde{\eta}^2],$$

$$c_3 = 1 - \tilde{\eta}^2/2. \tag{4.15}$$

Note $P_4(c) > 0$ for real solutions for z.

Field line examples

We integrate the field line equations, (4.7) for **B** given by (4.4) numerically as an initial value problem. If one uses the variables $(\tilde{x}, \tilde{y}, z)$, the field line equations reduce

https://doi.org/10.1017/S0022377811000420 Published online by Cambridge University Press

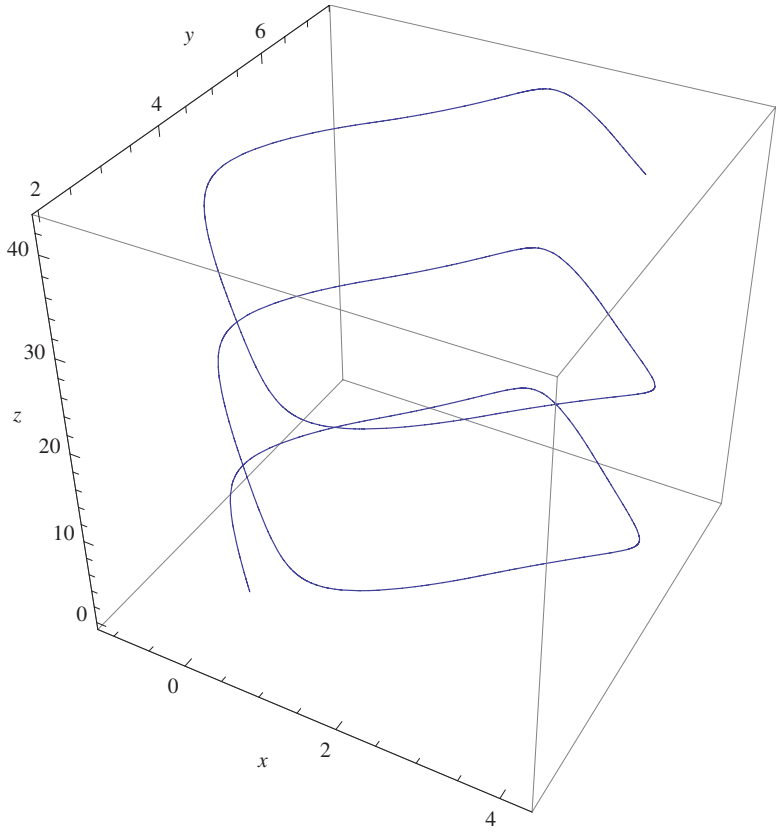


Figure 1. (Colour online) Field line for the double Alfvén wave (4.4) with $k_2 = k_1 = k = 1$. The parameter $\eta = 0.1$, $(\tilde{x}_0, \tilde{y}_0, z_0) = (-\pi/2, \arccos(-\eta/2), 0)$ are initial conditions. Note the rectangular shape of the helix.

to

$$\frac{d\tilde{x}}{ds} = \frac{k}{\sqrt{2}} \sin\tilde{y} \sin\tilde{x}, \quad \frac{d\tilde{y}}{ds} = \frac{k}{\sqrt{2}} \cos\tilde{x} \cos\tilde{y},$$

$$\frac{dz}{ds} = (\sin^2\tilde{x}\cos^2\tilde{y} + \sin^2\tilde{y}\cos^2\tilde{x})^{1/2}, \qquad (4.16)$$

where s is arc length along the field. Given $\tilde{\eta}$, we choose the starting point for the integration as $(\tilde{x}_0, \tilde{y}_0, z_0) = (-\pi/2, \arccos(-\tilde{\eta}/2), 0)$. Without loss of generality, we choose $k = 1$ and $\tilde{\eta} = \eta$. The field lines are determined by the value of η where $0 < \eta < 2$.

Figure 1, shows the magnetic field line integral solutions for the case $\eta = 0.1$, obtained by integrating (4.16). The field line is a helix along the z-axis in which the xy cross-section is roughly rectangular in shape, and symmetric about the $y = x$ line (note $kx = \tilde{x} + \tilde{y}$ and $ky = \tilde{y} - \tilde{x}$). Plots of x, y, and z versus s are displayed in Fig. 2. The plots of $x(s)$ and $y(s)$ show out of phase periodic solutions, but $z(s)$ is on average increasing monotonically, modulated by small ripples. The field line hodograph of $[B_x(s), B_y(s), B_z(s)]$ in the components $B_x(s)$, $B_y(s)$, and $B_z(s)$ are displayed in Fig. 3. Note that B_z has a repeating M type shape, with $B_z = 0$ at the points $(x, y) = (m\pi, n\pi)$ (m and n are integers). The field line hodograph of $[B_x(s), B_y(s), B_z(s)]$ in Fig. 4 consists of four arcs on the sphere $B = const.$, which are symmetric about the $y = x$ line. The hodograph, resembles two script Ms similar to the McDonald's restaurant symbol. Figure 5 shows that the hodograph of **B** in Fig. 4 lies on the sphere $|\mathbf{B}| = const$.

Figures 6–8 show the effect of decreasing η to $\eta = 0.01$. The field lines in Fig. 6 are similar to those in Fig. 1 (note $\eta = 0.1$ in Fig. 1). Figures 7 and 8 show the hodograph of **B**. Figures 7 and 8 show that the hodographs lie on the sphere $|\mathbf{B}| = const.$ and and are more concentrated about the north pole than for the case $\eta = 0.1$ illustrated in Figs. 1–5. In the limit as $\eta \to 0$ the hodographs become meridians, passing through the north pole, with projections $y = -x$ and $y = x$ on the xy-plane. Figures 9 and 10 show the field lines and hodograph for the case $\eta = 1$. Figures 11 and 12 show the field lines and hodograph for $\eta = 1.9$. Note that the amplitude of the oscillations of B_z in the hodographs decreases as η increases. One cannot visually see oscillations in B_z on the hodograph for $\eta = 1.9$ in Fig. 12. In the limit as $\eta \to 2$, the hodograph becomes a point at the north pole. There are no solutions possible for $\eta > 2$.

The hodograph for $\eta = 1.9$ appears in first order to be a circle at a constant latitude near the north pole. Note that a shear wave propagating along the z-axis, can be represented by a constant latitude circle on the $|\mathbf{B}| = const.$ sphere, where the radius of the circle is $B_\perp = B\cos\alpha$. The helical field lines in Figs. 9 and 10 become more circular with increasing η. The helical field lines in Figs. 1, 6, 9, and 11 are left-handed. By changing $\eta \to -\eta$ in these solutions gives right-handed helixes.

https://doi.org/10.1017/S0022377811000420 Published online by Cambridge University Press

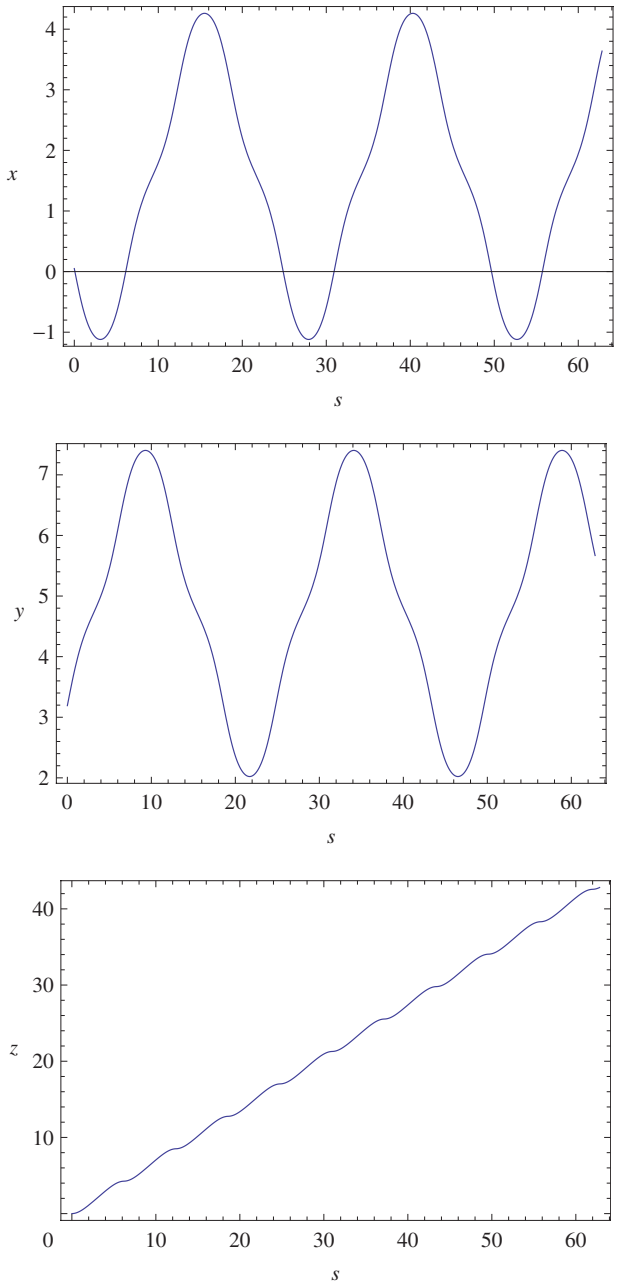


Figure 2. (Colour online) Field line coordinates $x(s)$, $y(s)$, and $z(s)$ versus distance s along the field line for the double Alfvén wave (4.4) with $k_2 = k_1 = k = 1$ and $\eta = 0.1$. The parameters are the same as in Fig. 1.

Examples in Figs. 1–12 assumed $k_1 = k_2$. For $k_1 \neq k_2$, the field line equations (4.4) can be written in the form:

$$\frac{d\bar{x}}{ds} = \frac{k_1}{\sqrt{2}}\cos(r\bar{y}), \quad \frac{d\bar{y}}{ds} = \frac{k_1}{\sqrt{2}}\cos(\bar{x}),$$
$$\frac{d\bar{z}}{ds} = \frac{k_1}{\sqrt{2}}[\sin^2(\bar{x}) + \sin^2(r\bar{y})]^{1/2}, \tag{4.17}$$

where

$$\bar{x} = k_1 x, \quad \bar{y} = k_1 y, \quad \bar{z} = k_1 z, \quad r = \frac{k_2}{k_1}. \tag{4.18}$$

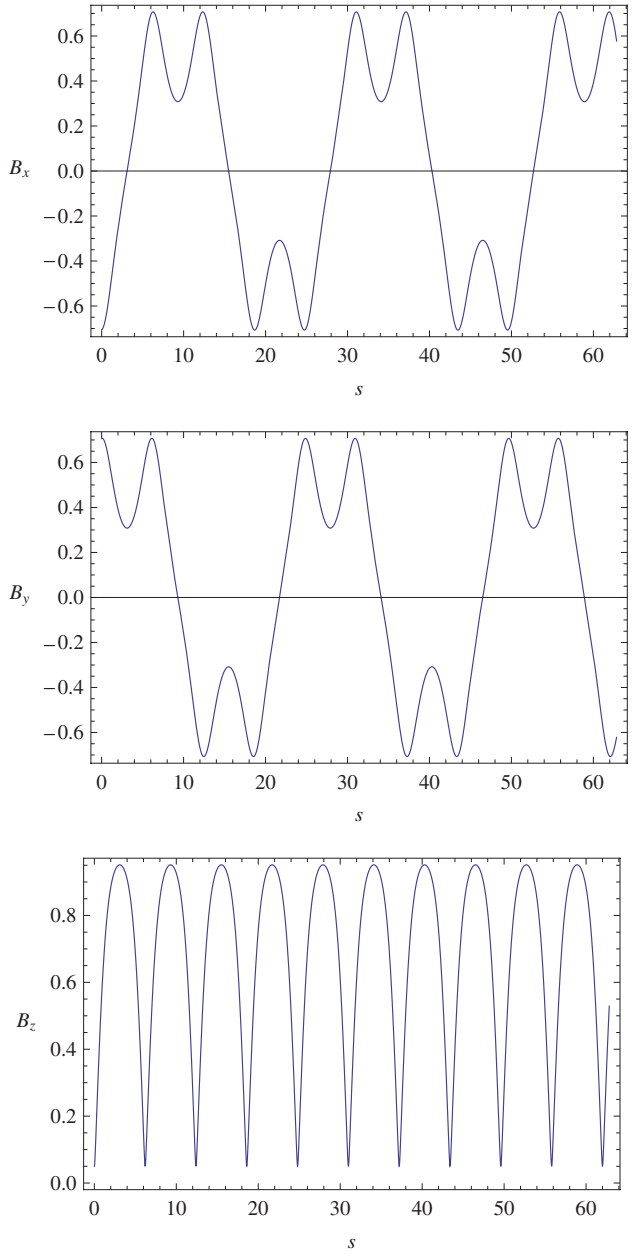


Figure 3. (Colour online) $[B_x(s), B_y(s), \text{and } B_z(s)]$ versus s of the magnetic field **B** for the double Alfvén wave solution (4.4), where s denotes distance along the field line. The parameters are the same as in Fig. 1.

The field line equations (4.17) possess the integral

$$\sin(\bar{x}) - \frac{\sin(r\bar{y})}{r} = \eta k_1 \equiv \bar{\eta}, \tag{4.19}$$

where η is the integration constant in (4.8).

Lump type distributions for $h(x)$ and $g(y)$ will give rise to a different class of solutions that are not periodic in x and y by choosing

$$h(x) = \frac{Nx}{x^2 + a^2}, \quad g(y) = \frac{Ny}{y^2 + b^2}. \tag{4.20}$$

The solution for **B** in (4.2) requires $h^2 + g^2 < 1$ in order for B_z to be real. Note that $|h|$ and $|g| \to 0$ as $\varpi = \sqrt{x^2 + y^2} \to \infty$ and the field $\mathbf{B} \to B(0, 0, 1)$ is uniform as $\varpi \to \infty$.

https://doi.org/10.1017/S0022377811000420 Published online by Cambridge University Press

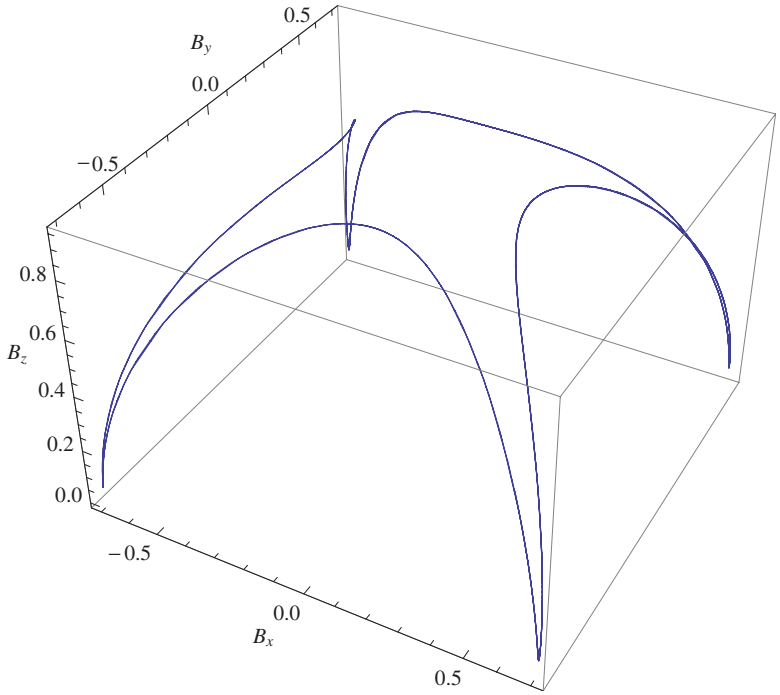


Figure 4. (Colour online) Hodograph of $[B_x(s), B_y(s), B_z(s)]$ of the magnetic field **B** for the double Alfvén wave solution (4.4), where s denotes distance along the field line. The parameters are the same as in Fig. 1.

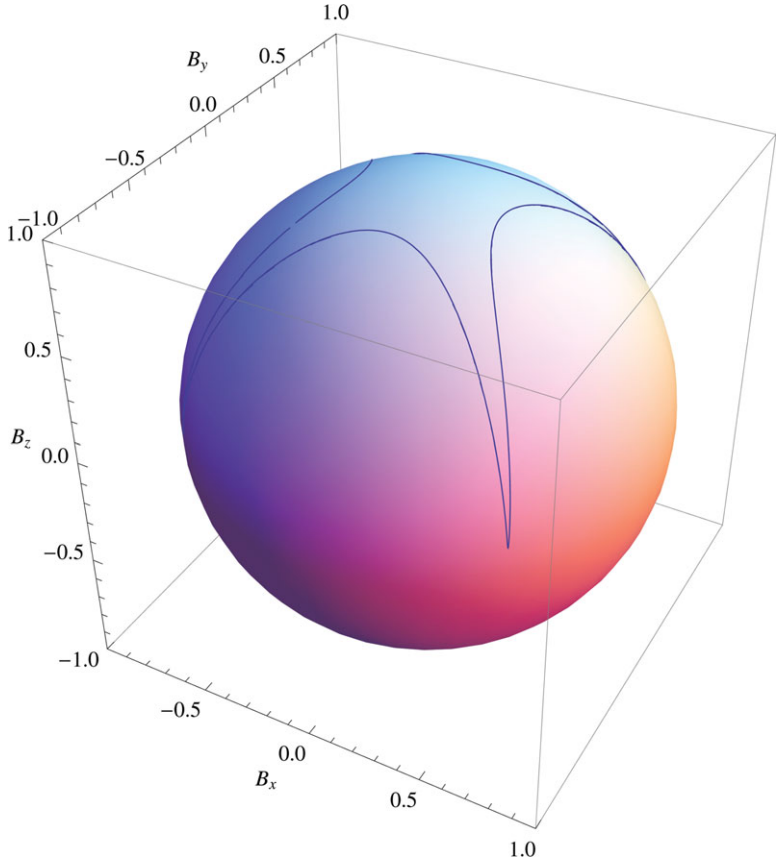


Figure 5. (Colour online) Hodograph of $[B_x(s), B_y(s), B_z(s)]$ of the magnetic field **B** for the double Alfvén wave solution (4.4), where s denotes distance along the field line. Note that the hodograph lies on the sphere $|\mathbf{B}| = const$. The parameters are the same as in Fig. 1.

https://doi.org/10.1017/S0022377811000420 Published online by Cambridge University Press

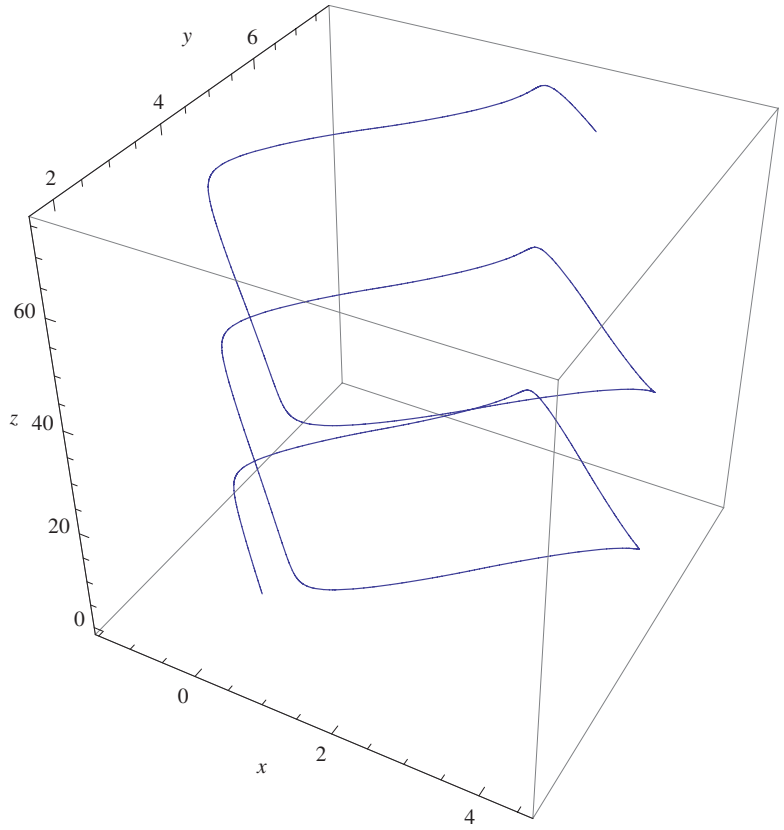


Figure 6. (Colour online) Field line for the double Alfvén wave (4.4) with $k_2 = k_1 = k = 1$. The parameter $\eta = 0.01$, $(\tilde{x}_0, \tilde{y}_0, z_0) = (-\pi/2, \arccos(-\eta/2), 0)$ are the initial conditions. Note the rectangular shape of the helix.

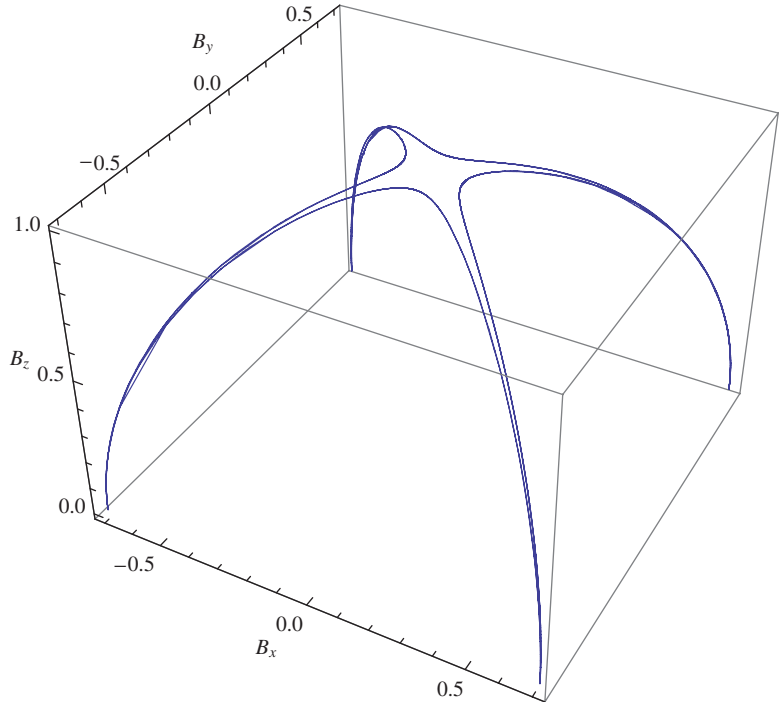


Figure 7. (Colour online) Hodograph of $[B_x(s), B_y(s), B_z(s)]$ of the magnetic field **B** for the double Alfvén wave solution (4.4) for the same parameter values as Fig. 6, where s denotes distance along the field line. Note that the hodograph lies on the sphere $|\mathbf{B}| = const.$

https://doi.org/10.1017/S0022377811000420 Published online by Cambridge University Press

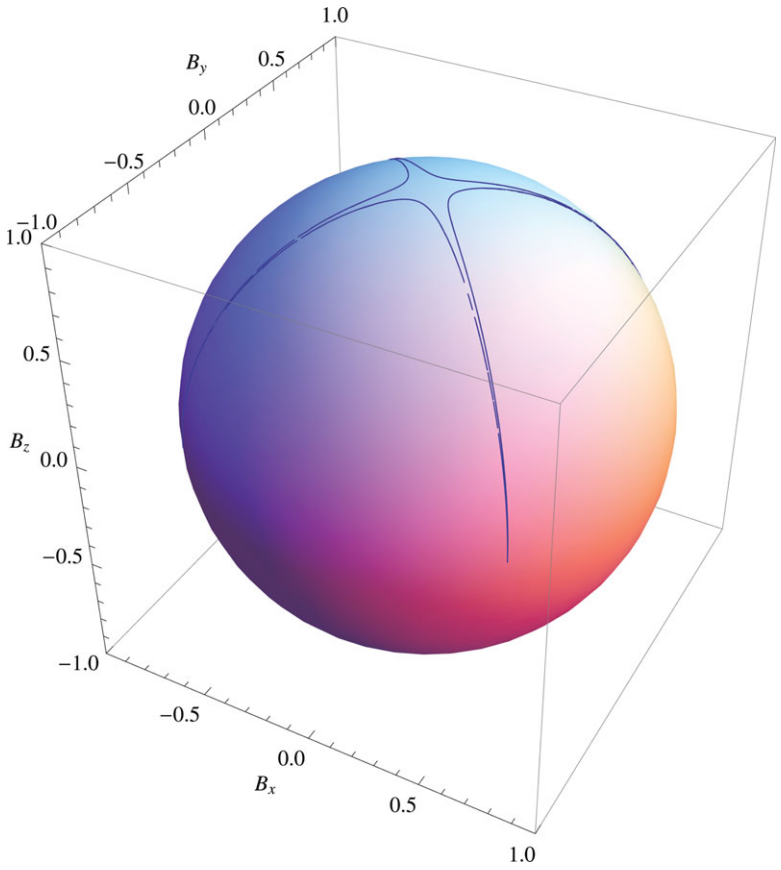


Figure 8. (Colour online) Hodograph of $[B_x(s), B_y(s), B_z(s)]$ of the magnetic field **B** for the double Alfvén wave solution (4.4), where s denotes distance along the field line. Note that the hodograph lies on the sphere $|\mathbf{B}| = const$. The parameters are the same as in Fig. 6.

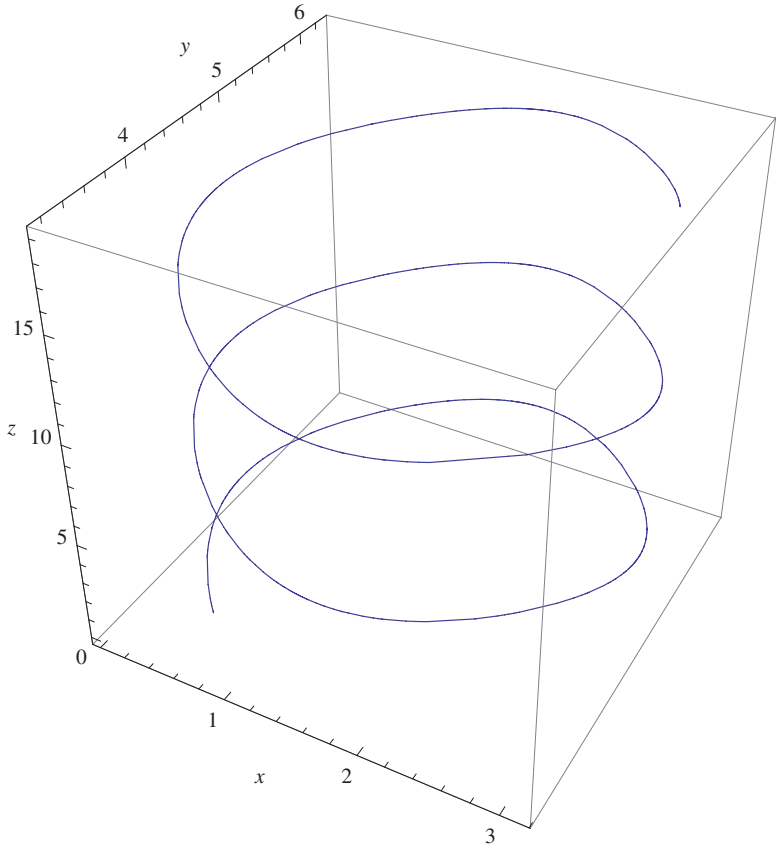


Figure 9. (Colour online) Field line for the double Alfvén wave (4.4) with $k_2 = k_1 = k = 1$. The parameter $\eta = 1.0$, $(\tilde{x}_0, \tilde{y}_0, z_0) = (-\pi/2, \arccos(-\eta/2), 0)$ are the initial conditions.

https://doi.org/10.1017/S0022377811000420 Published online by Cambridge University Press

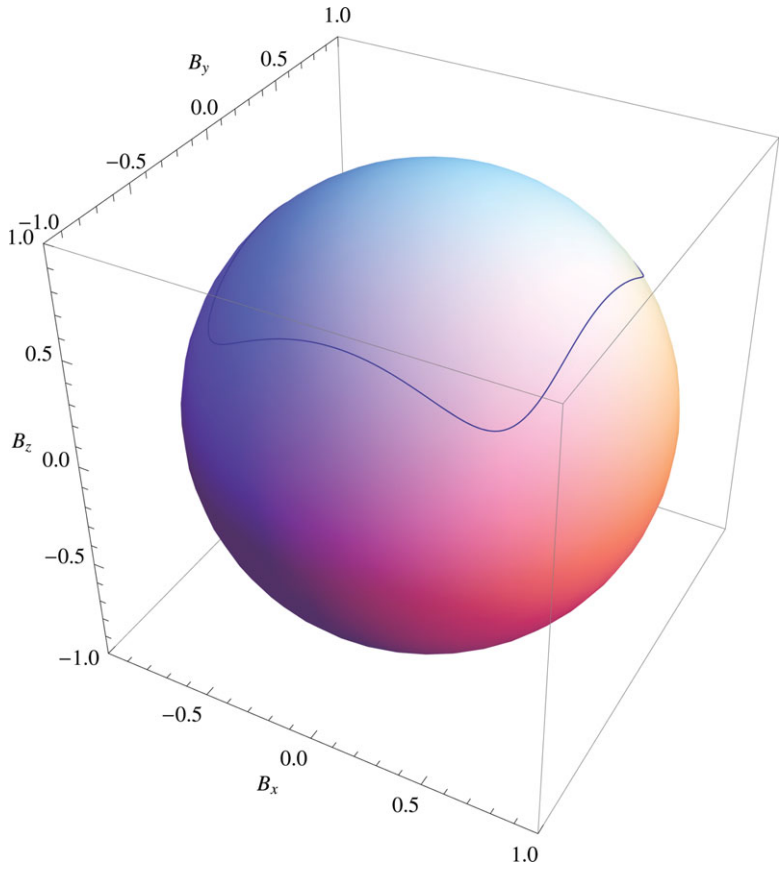


Figure 10. (Colour online) Hodograph of $[B_x(s), B_y(s), B_z(s)]$ of the magnetic field **B** for the double Alfvén wave solution (4.4), where s denotes distance along the field line. Note that the hodograph lies on the sphere $|\mathbf{B}| = const.$ $\eta = 1.0$. The parameters are the same as in Fig. 9.

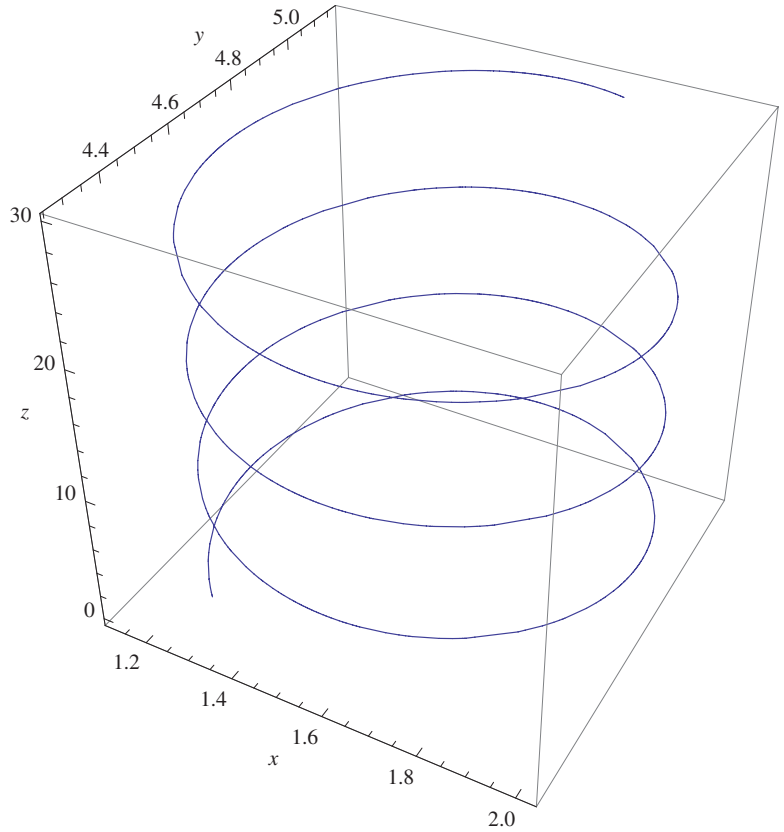


Figure 11. (Colour online) Field line for the double Alfvén wave (4.4) with $k_2 = k_1 = k = 1$. The parameter $\eta = 1.9$, $(\tilde{x}_0, \tilde{y}_0, z_0) = (-\pi/2, \arccos(-\eta/2), 0)$ are the initial conditions.

https://doi.org/10.1017/S0022377811000420 Published online by Cambridge University Press

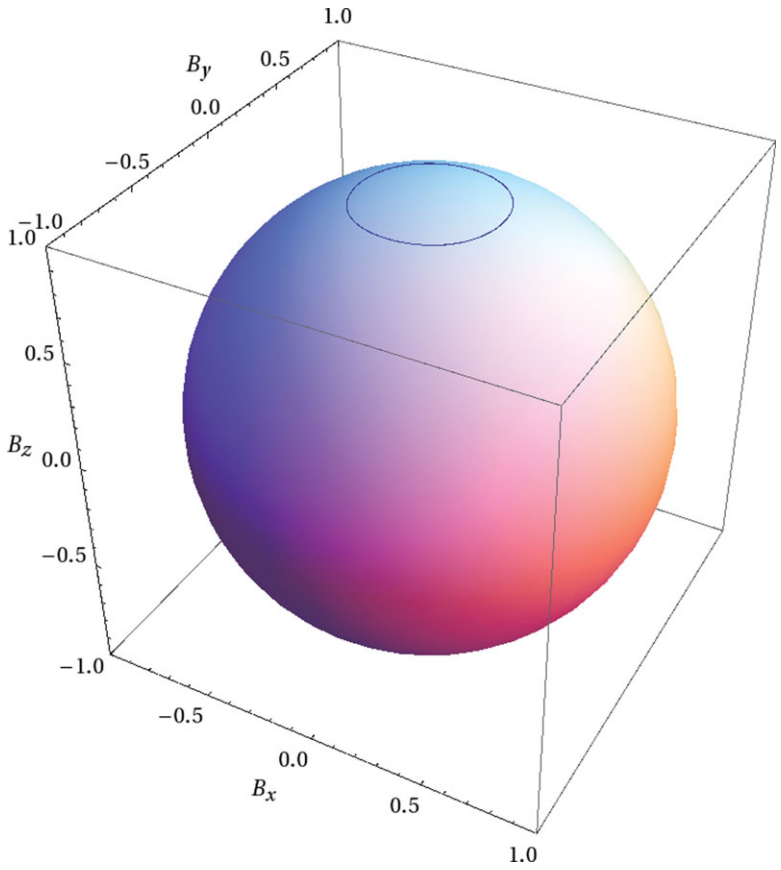


Figure 12. (Colour online) Hodograph of $[B_x(s), B_y(s), B_z(s)]$ of the magnetic field $\mathbf{B}$ for the double Alfvén wave solution (4.4), where s denotes distance along the field line. Note that the hodograph lies on the sphere $|\mathbf{B}| = const.$ $\eta = 1.9$. The parameters are the same as in Fig. 11.

5. The Frenet–Serret equations and Hamiltonians

In this section, we indicate extensions of the theory of simple and double Alfvén waves, which require further development. Section 5.1 describes the Hamiltonian formulation of simple Alfvén waves. Some of the complications of the theory for double Alfvén waves are indicated in Sec. 5.2. A detailed exposition of these ideas lies beyond the scope of the present paper.

5.1. Simple Alfvén waves

It was shown by Webb et al. (2011) that $\mathbf{B}(\varphi)$ for Alfvén simple waves satisfies the evolution equation

$$\frac{d\mathbf{B}}{d\varphi} = \alpha(\varphi)\mathbf{n} \times \mathbf{B}, \tag{5.1}$$

where φ is the simple wave phase and $\mathbf{n}(\varphi)$ is the wave normal. Webb et al. (2011) introduced the abstract curve $\mathbf{x} = \mathbf{X}(\varphi)$ with tangent vector $\mathbf{n} = \mathbf{X}'(\varphi)/|\mathbf{X}'(\varphi)|$ to describe the wave in which

$$\mathbf{e}_1 = \frac{\mathbf{X}'(\varphi)}{|\mathbf{X}'(\varphi)|} = \mathbf{n}(\varphi), \quad \mathbf{e}_2 = \frac{\mathbf{e}_1'(\varphi)}{|\mathbf{e}_1'(\varphi)|}, \quad \mathbf{e}_3 = \mathbf{e}_1 \times \mathbf{e}_2 \tag{5.2}$$

are the tangent vector, principal normal, and bi-normal to the curve $\mathbf{x} = \mathbf{X}(\varphi)$. The magnetic field induction $\mathbf{B}$ in the wave is written in the form:

$$\mathbf{B}(\varphi) = B^1\mathbf{e}_1 + B^2\mathbf{e}_2 + B^3\mathbf{e}_3. \tag{5.3}$$

The Frenet–Serret equations for the moving tri-hedron $\{\mathbf{e}_1, \mathbf{e}_2, \mathbf{e}_3\}$ (e.g. Struick 1961; Lipschutz 1969) are

$$\frac{d\mathbf{e}_1}{d\varphi} = \kappa\mathbf{e}_2, \quad \frac{d\mathbf{e}_2}{d\varphi} = -\kappa\mathbf{e}_1 + \tau\mathbf{e}_3, \quad \frac{d\mathbf{e}_3}{d\varphi} = -\tau\mathbf{e}_2, \tag{5.4}$$

where $\kappa(\varphi)$ and $\tau(\varphi)$ are respectively the curvature and torsion coefficients for the curve. The Frenet–Serret equations (5.4) can be written in the matrix form:

$$\frac{d}{d\varphi}\begin{pmatrix}\mathbf{e}_1\\ \mathbf{e}_2\\ \mathbf{e}_3\end{pmatrix} = \begin{pmatrix}\mathsf{O}_3 & \kappa\mathsf{I}_3 & \mathsf{O}_3\\ -\kappa\mathsf{I}_3 & \mathsf{O}_3 & \tau\mathsf{I}_3\\ \mathsf{O}_3 & -\tau\mathsf{I}_3 & \mathsf{O}_3\end{pmatrix}\begin{pmatrix}\mathbf{e}_1\\ \mathbf{e}_2\\ \mathbf{e}_3\end{pmatrix} \equiv \mathsf{J}\begin{pmatrix}\mathbf{e}_1\\ \mathbf{e}_2\\ \mathbf{e}_3\end{pmatrix}, \tag{5.5}$$

or in the vector form:

$$\frac{d\mathbf{e}_\alpha}{d\varphi} = \mathbf{D} \times \mathbf{e}_\alpha, \tag{5.6}$$

where

$$\mathbf{D} = \tau\mathbf{e}_1 + \kappa\mathbf{e}_3, \tag{5.7}$$

is the Darboux vector or twist vector for the curve $\mathbf{X}(\varphi)$.

The Frenet–Serret equations (5.5) may also be written in the Hamiltonian form (Padhye 1998):

$$\frac{dz^i}{d\varphi} = \{z^i, H\} = J^{ij}\frac{\partial H}{\partial z^j}, \tag{5.8}$$

where $\mathbf{z} = (\mathbf{e}_1^T, \mathbf{e}_2^T, \mathbf{e}_3^T)^T$ is a nine-dimensional vector describing the moving trihedron $\{\mathbf{e}_1, \mathbf{e}_2, \mathbf{e}_3\}$ and the $9 \times$

https://doi.org/10.1017/S0022377811000420 Published online by Cambridge University Press

9 skew-symmetric matrix J is defined in (5.5). The Hamiltonian for the Frenet–Serret equations is

$$H = \frac{1}{2}(\alpha^2 + \beta^2 + \gamma^2), \tag{5.9}$$

where

$$\alpha^i = e_1^i, \quad \beta^i = e_2^i, \quad \gamma^i = e_3^i \tag{5.10}$$

are the Cartesian components of $\mathbf{e}_1$, $\mathbf{e}_2$, and $\mathbf{e}_3$. The Poisson bracket for the Hamiltonian system is

$$\{F, G\} = \frac{\partial F}{\partial z^i} J^{ij} \frac{\partial G}{\partial z^j}. \tag{5.11}$$

The Poisson bracket (5.11) is skew symmetric and satisfies the Jacobi identity. However, the symplectic matrix J is 'time-dependent' as it depends on the curvature and torsion coefficients $\kappa(\varphi)$ and $\tau(\varphi)$. The Hamiltonian H is 'time-independent' as $dH/d\varphi = 0$. The Casimirs for the bracket (5.11) satisfy $\{C, f\} = 0$ for arbitrary function $f(z)$ of the dependent variable z, implies $J^{ij}C_{z^j} = 0$. The Casimirs are arbitrary functions of the form $C(\tau\alpha + \kappa\gamma)$. If κ and τ are constants (i.e. the curve is a helix), then C is a constant. For κ or τ functions of φ, the Casimirs are not constants (Padhye 1998). Odd dimensional Hamiltonian systems have Casimirs (Morrison 1998).

From (5.3),

$$\frac{d\mathbf{B}}{d\varphi} = \left(\frac{dB^1}{d\varphi} - \kappa B^2\right)\mathbf{e}_1 + \left(\frac{dB^2}{d\varphi} + \kappa B^1 - \tau B^3\right)\mathbf{e}_2 + \left(\frac{dB^3}{d\varphi} + \tau B^2\right)\mathbf{e}_3. \tag{5.12}$$

Using (5.1) for the evolution of $\mathbf{B}$ follows that the components (B^1, B^2, B^3) in the Frenet frame also satisfy a modified form of the Frenet–Serret equations:

$$\frac{d}{d\varphi}\begin{pmatrix} B^1 \\ B^2 \\ B^3 \end{pmatrix} = \begin{pmatrix} 0 & \kappa & 0 \\ -\kappa & 0 & \tilde{\tau} \\ 0 & -\tilde{\tau} & 0 \end{pmatrix}\begin{pmatrix} B^1 \\ B^2 \\ B^3 \end{pmatrix} \equiv \mathsf{J}_B \begin{pmatrix} B^1 \\ B^2 \\ B^3 \end{pmatrix}, \tag{5.13}$$

where

$$\tilde{\tau} = \tau(\varphi) - \alpha(\varphi), \tag{5.14}$$

is a modified torsion coefficient, taking into account the torsion parameter $\alpha(\varphi)$ for magnetic field. From Webb et al. (2010),

$$\alpha(\varphi) = -\frac{\mu H_J}{|\nabla\varphi|B_\perp^2} \equiv -\mathbf{J}\cdot\mathbf{e}_B \frac{\mu B}{|\nabla\varphi|B_\perp^2}, \tag{5.15}$$

where $\mathbf{J} = \nabla \times \mathbf{B}$ is the current and $h_J = \mathbf{J}\cdot\mathbf{B}$ is the current helicity, which is equal to the product of B and the field aligned current $\mathbf{J}\cdot\mathbf{e}_B$. It is clear from (5.13)–(5.15) that $(B^1, B^2, B^3)^T$ evolves according to the Hamiltonian equations:

$$\frac{dB^\alpha}{d\varphi} = \{B^\alpha, H_B\}_B = J_B^{\alpha\beta}\frac{\partial H_B}{\partial B^\beta}, \tag{5.16}$$

where J_B is the symplectic operator or matrix in (5.13) and

$$H_B = \frac{1}{2}[(B^1)^2 + (B^2)^2 + (B^3)^2] \tag{5.17}$$

is the Hamiltonian. The Poisson bracket $\{F, G\}_B$ in (5.16) is given by (5.11) except that the phase space is now three dimensional and J is replaced by J_B.

Since the matrices J and J_B have zero determinant, these matrices are not invertible, and hence the Frenet system (5.5) and the magnetic field evolution system (5.16) should more properly be referred to as the semi-Hamiltonian systems.

A variational and Hamiltonian formulation of the Frenet frame base vectors $\{\mathbf{e}_1, \mathbf{e}_2, \mathbf{e}_3\}$ and (B^1, B^2, B^3) can be developed by using a stereographic projection of a point (u, v, w) on the unit sphere passing through the north pole on the sphere, onto the horizontal (u, v)-plane to obtain a complex Riccati equation. The Riccati equation, in turn, can be reduced to a second-order linear differential equation by using the Cole–Hopf-type transformation (Eisenhart 1960).

5.2. Double Alfvén waves

For double Alfvén waves, the Hamiltonian for $\mathbf{B}$ is again $H_B = 1/2B^2$, except that now there are two 'time-evolution' variables φ^1 and φ^2. The two evolutions must satisfy the compatibility conditions $\mathbf{B}_{\varphi^1\varphi^2} = \mathbf{B}_{\varphi^2\varphi^1}$. There are two natural Frenet–Serret frames to describe the φ^1 and φ^2 evolutions. The base vectors for these two frames are related by an orthogonal transformation matrix O. There are other orthonormal frames in which the φ^1 and φ^2 evolutions can be described by the use of the non-canonical Poisson brackets.

The detailed theory for double Alfvén waves is fairly complicated. It involves the possibility that the wave normals $\mathbf{n}^1(\varphi^1, \varphi^2)$ and $\mathbf{n}^2(\varphi^1, \varphi^2)$ are tangent to the abstract two-dimensional surface $\mathbf{r} = \mathbf{r}(\varphi^1, \varphi^2)$ in three dimensions, in which $\mathbf{n}^3 = \mathbf{n}^1 \times \mathbf{n}^2$ is normal to the surface, i.e.

$$\mathbf{n}^1 = \mathbf{r}_{\varphi^1} \quad \text{and} \quad \mathbf{n}^2 = \mathbf{r}_{\varphi^2}. \tag{5.18}$$

Thus, the theory involves the classical theory of two-dimensional surfaces embedded in a three-dimensional Euclidean manifold described by differential geometry. This involves the first and second fundamental forms for the surface, and the Gauss–Weingarten equations and the Mainardi-Codazzi compatibility equations for the surface (e.g. Struick 1961; Rogers and Schief 2002). This theory can be developed using Cartan's method of moving frames and differential forms (e.g. Flanders 1963; Frankel 1997). A more complete exposition of these ideas lies beyond the scope of the present paper.

6. Summary and concluding remarks

We have investigated the double Alfvén waves in MHD, based on the work of Grundland and Picard (2004) on double waves in MHD and on ideas on MHD simple waves (Webb et al. 1996, 2010, 2011).

Examples of double Alfvén waves with two independent constant wave normals $\mathbf{n}^1$ and $\mathbf{n}^2$ (Sec. 4) were obtained. Numerical examples of the field lines

https://doi.org/10.1017/S0022377811000420 Published online by Cambridge University Press

and hodographs of $\mathbf{B}$ for $\mathbf{n}^1$ and $\mathbf{n}^2$ constant vectors were obtained (Sec. 5). The hodographs of $\mathbf{B}$ show that the tip of the magnetic field vector moves on the surface of a sphere of radius $|\mathbf{B}| = const$. The wave torsion coefficients $\mu(\varphi^1, \varphi^2)$ and $\nu(\varphi^1, \varphi^2)$ are complicated functions of φ^1 and φ^2.

Extensions of the theory of simple and double waves were discussed (Sec. 5). A Hamiltonian formulation of simple Alfvén waves is given in Sec. 5.1. The extension of the theory of double Alfvén waves is discussed in Sec. 5.2. This involves the differential geometry of two-dimensional surfaces in the Euclidean 3-space E^3

The double Alfvén wave solutions investigated in this paper are for constant wave normals $\mathbf{n}^1$ and $\mathbf{n}^2$. More general solutions in which the wave normals are non-trivial functions of φ^1 and φ^2 are of interest.

Evidence of the nonlinear Alfvénic structures in the solar wind were given by Roberts et al. (1987), Bruno et al. (2001), Bruno and Carbone (2005), and Gosling et al. (2009, 2010). Bruno et al. (2001) and Bruno and Carbone (2005) present hodographs of the magnetic field $\mathbf{B}$ in which the tip of the magnetic field vector $\mathbf{B}$ moves over the surface of a sphere of radius $B \approx const.$, as expected for nonlinear Alfvén waves.

Acknowledgements

GMW and GPZ were supported in part by NASA grants NN05GG83G and NSF grant nos. ATM-03-17509 and ATM-04-28880. QH, BD, and GMW were supported in part by NASA grants NNX07AO73G and NNX10AG03G and NSF SHINE, AGS-1062050.

References

Barnes, A. 1976 On the non-existence of plane polarized large amplitude Alfvén waves. *J. Geophys. Res.* **81**(1), 281–282.

Barnes, A. 1981 Interplanetary Alfvénic fluctuations: a stochastic model. *J. Geophys. Res.* **86**(A9), 7498–7506.

Barnes, A. and Hollweg, J. V. 1974 Large amplitude hydromagnetic waves. *J. Geophys. Res.* **79**, 2302–2318.

Breech, B., Matthaeus, W. H., Minnie, J., Bieber, J. W., Oughton, S., Smith, C. W. and Isenberg, P. A. 2008 Turbulence transport throughout the heliosphere. *J. Geophys. Res.* **113**, A08105. doi:10.1029/2007JA012711.

Bruno, R. and Carbone, V. 2005 The solar wind as a turbulence laboratory, In *Living Reviews in Space Physics.* http:/www.livingreviews.org/lrsp-2005-4

Bruno, R., Carbone, V., Veltri, P., Pietropaolo, E. and Bavassano, B. 2001 Identifying intermittency events in the solar wind. *Planet. Space Sci.* **49**, 1201–1210.

Chen, L. and Hasegawa, A. 1974 Plasma heating by spatial resonance of Alfvén waves. *Phys. Fluids* **17**(7), 1399–1403.

Eisenhart, L. P. 1960 *A Treatise on the Differential Geometry of Curves and Surfaces.* New York: Dover (re-publication of 1909 edition by Ginn and Co.).

Flanders, H. 1963 *Differential Forms with Applications to the Physical Sciences.* New York: Academic.

Frankel, T. 1997 *The Geometry of Physics, An Introduction.* Cambridge, UK: Cambridge University Press, p. 161, formula (5.6).

Gekelman, W., Vicenza, S., Van Compernolle, B., Morales, G. J., Maggs, J. E., Prybyl, P. and Carter, T. A. 2011 The many faces of shear Alfvén waves. *Phys. Plasmas* **18**, 08511, doi:10.1063/1.3592210.

Gosling, J. T., McComas, D. J., Roberts, D. A. and Skoug, R. M. 2009 A one-sided aspect of Alfvénic fluctuations in the solar wind. *Astrophys. J.* **695**, L213–L216.

Gosling, J. T., Teh, W. L. and Eriksson, S. 2010(August 10) A torsional Alfvén wave embedded within a small magnetic flux rope in the solar wind. *Ap. J. Lett.* **719**, L36–L40, doi:10.1088/2041-8205/719/1/L36.

Grundland, A. M. and Huard, B. 2007 Conditional symmetries and Riemann invariants for hyperbolic systems of PDEs. *J. Phys. A: Math. Theor.* **40**, 4093–4123, doi:10.1088/1751-8113/40/15/004.

Grundland, A. M. and Picard, P. 2004 On conditionally invariant solutions of magnetohydrodynamic equations multiple waves. *J. Nonlinear Math. Phys.* **11**(1), 47–74.

Hasegawa, A. and Chen, L. 1975 Kinetic process of plasma heating due to Alfvén wave excitation. *Phys. Rev. Lett.* **35**(6), 370–373.

Heinemann, M. and Olbert, S. 1980 Non-WKB Alfvén waves in the solar wind. *J. Geophys. Res.* **85**, 1311.

Lipschutz, M. 1969 *Theory and Problems of Differential Geometry* (Schaum Outline Series). New York: McGraw Hill.

MacGregor, K. B. and Charbonneau, P. 1994 Stellar winds with non-WKB Alfvén waves I: wind models for solar coronal conditions. *Astrophys. J.* **430**, 387–398.

Matthaeus, W. H. and Goldstein, M. L. 1982 Measurement of the rugged invariants of magnetohydrodynamic turbulence in the solar wind. *J. Geophys. Res.* **87**(A8), 6011–6028.

Matthaeus, W. H., Oughton, S., Pontius, Jr, D. H. and Zhou, Y. 1994 Evolution of energy containing eddies in the solar wind. *J. Geophys. Res.* **A10**, 19267–19287.

Morrison, P. J. 1998 Poisson brackets for fluids and plasmas. *Rev. Mod. Phys.* **70**, 467–521.

Padhye, N. S. 1998 Topics in Lagrangian and Hamiltonian fluid dynamics: relabeling symmetry and ion acoustic wave stability. *PhD Dissertation*, University of Texas at Austin.

Roberts, D. A., Klein, L. W., Goldstein, M. L. and Matthaeus, W. H. 1987 The nature and evolution of magnetohydrodynamic fluctuations in the solar wind: Voyager observations. *J. Geophy. Res.* **92**, 11021.

Rogers, C. and Schief, W. K. 2002 *Bäcklund and Darboux Transformations, Geometry and Modern Apllications in Soliton Theory.* Cambridge UK: Cambridge University Press.

Struick, D. J. 1961 *Lectures on Classical. Differential Geometry*, 2nd edn. Reading, MA: Addison-Wesley.

Webb, G. M., Ratkiewicz, R., Brio, M. and Zank, G. P. 1996 Multi-dimensional MHD simple waves. In: *Solar Wind 8, AIP Conf. Proc.*, Vol. 382 (ed. D. Winterhalter, J. T. Gosling, S. R. Habbal, W. S. Kurth and M. Neugebauer). New York: AIP, pp. 335–338.

Webb, G. M. and Zank, G. P. 2007 Fluid relabelling symmetries, Lie point symmetries and the Lagrangian map in magnetohydrodynamics and gas dynamics. *J. Phys. A. Math. Theor.* **40**, 545–579, doi:10.1088/1751-8113/40/3/013.

Webb, G. M., Hu, Q., Dasgupta, B., Roberts, D. A. and Zank, G. P. 2010 Alfven simple waves: Euler potentials

https://doi.org/10.1017/S0022377811000420 Published online by Cambridge University Press

and magnetic helicity. *Astrophys. J.* **725**, 2128–2151, doi:10.1088/0004-637X/725/2/2128.

Webb, G. M., Zank, G. P., Burrows, R. H. and Ratkiewicz, R. E. 2011 Simple Alfvén waves. *J. Plasma Phys.* **77**(part 1), 51–93, doi:10.101/S00233377809990596.

Zank, G. P., Hunana, P., Shaikh, D., Florinski, V. and Webb, G. M. 2010 The transport of low-frequency turbulence throughout the heliosphere. *AIP Proc. Conf.* **1302**, 167–173.

Zank, G. P., Matthaeus, W. H. and Smith, C. W. 1996 Evolution of turbulent magnetic fluctuation power with heliocentric distance. *J. Geophys. Res.* **101**, 17801.

Zhou, Y. and Matthaeus, W. H. 1990a Transport and turbulence modeling of solar wind fluctuations. *J. Geophys. Res.* **95**, 10291.

Zhou, Y. and Matthaeus, W. H. 1990b Models of inertial range spectra of interplanetary magnetohydromagnetic turbulence. *J. Geophys. Res.* **95**(A9), 14881–14892.

https://doi.org/10.1017/S0022377811000420 Published online by Cambridge University Press